

Simultaneous generation of ultrahigh pressure and temperature to 50 GPa and 3300 K in multi-anvil apparatus

Cite as: Rev. Sci. Instrum. **92**, 103902 (2021); <https://doi.org/10.1063/5.0059279>

Submitted: 08 June 2021 • Accepted: 10 September 2021 • Published Online: 05 October 2021

 Longjian Xie, Artem Chanyshv, Takayuki Ishii, et al.



View Online



Export Citation



CrossMark

ARTICLES YOU MAY BE INTERESTED IN

[A simplified rapid-quench multi-anvil technique](#)

Review of Scientific Instruments **92**, 113902 (2021); <https://doi.org/10.1063/5.0062525>

[A rapid-quench technique for multi-anvil high-pressure-temperature experiments](#)

Review of Scientific Instruments **91**, 065105 (2020); <https://doi.org/10.1063/5.0005936>

[Internal resistive heating of non-metallic samples to 3000#K and >60#GPa in the diamond anvil cell](#)

Review of Scientific Instruments **92**, 063904 (2021); <https://doi.org/10.1063/5.0038917>

Time Stamping Event Detector



Position Sensitive · Time Sensitive · Event Driven · Portable

asa AMSTERDAM
SCIENTIFIC
INSTRUMENTS

www.amscins.com

I want to know more

Simultaneous generation of ultrahigh pressure and temperature to 50 GPa and 3300 K in multi-anvil apparatus

Cite as: Rev. Sci. Instrum. 92, 103902 (2021); doi: 10.1063/5.0059279

Submitted: 8 June 2021 • Accepted: 10 September 2021 •

Published Online: 5 October 2021



Longjian Xie,^{1,2,a)} Artem Chanyshv,^{1,3} Takayuki Ishii,^{1,4} Dmitry Bondar,¹ Keisuke Nishida,¹ Zhen Chen,⁴ Shrikant Bhat,³ Robert Farla,³ Yuji Higo,⁵ Yoshinori Tange,⁵ Xiaowan Su,⁶ BingMin Yan,⁴ Shuailin Ma,^{3,4} and Tomoo Katsura¹

AFFILIATIONS

¹ Bayerisches Geoinstitut, University of Bayreuth, 95440 Bayreuth, Germany

² Earth and Planetary Laboratory, Carnegie Institute for Science, Washington, DC 20015-1305, USA

³ Deutsches Elektronen-Synchrotron DESY, 22607 Hamburg, Germany

⁴ Center for High Pressure Science and Technology Advanced Research, Beijing 100094, China

⁵ Japan Synchrotron Radiation Research Institute, 1-1-1 Kouto, Sayo, Hyogo 689-5198, Japan

⁶ School of Earth and Space Sciences, Peking University, Beijing 100871, China

^{a)} Author to whom correspondence should be addressed: ddtuteng@gmail.com. Tel.: +49 (0)921 55 3743. Fax: +49 (0)921 55 3769.

ABSTRACT

We attempted to generate ultrahigh pressure and temperature simultaneously using a multi-anvil apparatus by combining the technologies of ultrahigh-pressure generation using sintered diamond (SD) anvils, which can reach 120 GPa, and ultrahigh-temperature generation using a boron-doped diamond (BDD) heater, which can reach 4000 K. Along with this strategy, we successfully generated a temperature of 3300 K and a pressure of above 50 GPa simultaneously. Although the high hardness of BDD significantly prevents high-pressure generation at low temperatures, its high-temperature softening allows for effective pressure generation at temperatures above 1200 K. High temperature also enhances high-pressure generation because of the thermal pressure. We expect to generate even higher pressure in the future by combining SD anvils and a BDD heater with advanced multi-anvil technology.

Published under an exclusive license by AIP Publishing. <https://doi.org/10.1063/5.0059279>

I. INTRODUCTION

The lower mantle occupies 56 vol. % of the whole Earth and is at high pressures from 23 to 136 GPa¹ and high temperatures from 1900 to 3600–5000 K.^{2–4} Therefore, the physicochemical properties of lower-mantle minerals and rocks have to be determined under these extreme conditions. Such data help us to interpret geophysical data and understand the composition, dynamics, and evolution of the lower mantle. The multi-anvil apparatus, especially combined with synchrotron x ray, is a powerful tool for such high-pressure–temperature experiments because of relatively large sample volumes and a homogeneous pressure–temperature field.⁵

The pressure and temperature ranges that can be generated using the multi-anvil apparatus are, however, limited. Conventional multi-anvil experiments can generate pressures and temperatures

only up to 25 GPa and 2500 K, respectively, which cover just the topmost part of the lower mantle conditions. Hereafter, we call higher pressure and temperature generations ultrahigh pressure and temperature. The pressure is limited mainly by the limited hardness (Vickers hardness < 2000) of a second-stage anvil material, i.e., conventional tungsten carbide (such as TF08, Fujilloy Co. Ltd., Japan). The temperature is limited mainly by the heating elements, which are LaCrO₃ and Re at pressures above 10 GPa. In addition, these heating elements bear another disadvantage of their opacity, even to high-energy synchrotron x rays, which becomes essential in identifying phases and measuring sample pressures *in situ*.

During the last decades, the pressure range generated using the multi-anvil apparatus has been expanded significantly, e.g., Refs. 6–9. The pressure was extended to 65 GPa using hard tapered WC anvils (TJS01, Fujilloy Co. Ltd., Japan) at room

temperatures.^{10,11} Thanks to the use of sintered diamond (SD), which has a higher hardness than WC, as an anvil material, pressure generation to 60 GPa was routinely performed.⁷ By the most advanced technique, the maximum pressure reached 120 GPa,⁹ which is close to the core-mantle boundary pressure. However, high-temperature generation has been limited to 1700–2300 K in these ultrahigh-pressure experiments.^{12,13}

Recently, a boron-doped diamond (BDD) has been developed as a new heater material. The BDD heater was originally developed using a graphite–boron composite as a precursor that converts to BDD *in situ* during the heating process.^{14–17} Later developments focused on the pre-sintered BDD heater, which has a better heating performance due to the avoidance of graphite-to-diamond conversion. For example, a BDD heater synthesized at high pressure and temperature expanded the temperature range to 4000 K at 15 GPa.¹⁸ In addition, the adoption of BDD synthesized by the chemical vapor deposition (CVD) method^{19,20} and the development of machinable BDD block²¹ made it possible to use BDD as a routine heating element in multi-anvil apparatus. Owing to its high x-ray transparency, BDD also shows a great advantage for *in situ* multi-anvil experiments. It enables various synchrotron-based studies such as determinations of phase relations and equations of state of minerals by x-ray diffraction (see the review in Ref. 22), viscosity measurement by x-ray radiography, e.g., Refs. 23 and 24, and measurement of liquid density by x-ray absorption, e.g., Refs. 25 and 26.

Simultaneous generation of ultrahigh pressures and temperatures should be one of the future directions of multi-anvil technical development. One promising idea is to combine the technologies of SD anvils and BDD heaters. However, there are two major difficulties in realizing this idea. One is the high thermal conductivity of SD, which would hinder ultrahigh-temperature generation because significantly high power supply is necessary. The other is the pressure support by the high strength of BDD, which may prevent ultrahigh-pressure generation.

In this study, we overcome the above two difficulties and simultaneously generated an ultrahigh pressure of 53 GPa at a temperature of 3300 K by combining the SD anvils and BDD heaters.

II. EXPERIMENTAL

In order to measure the pressure *in situ* with synchrotron x ray, high-pressure and high-temperature experiments were carried out in the beamline BL04B1 at SPring-8, Japan, and the beamline P61B of PETRA-III at DESY, Germany. Ge solid-state detectors (Ge-SSDs) were used to obtain energy-dispersive x-ray diffraction patterns of the MgO pressure marker. At the start of each beam time, the channel to the energy relationship of the Ge-SSDs was calibrated using γ rays of ¹³³Ba (53.16, 79.61, and 81.00 keV), ⁵⁷Co (14.41, 122.06, 136.47 keV), and ⁵⁵Fe (5.89 keV, only at SPring 8). The detector was positioned roughly at 6°. Then, prior to compression of each experiment, the precise angle (to four decimal places) was determined by x-ray diffraction on MgO inside the assembly under ambient conditions of room pressure and temperature. Incident x rays with the horizontal and vertical widths of 0.05 and 0.1 mm, respectively, were used to irradiate the pressure marker. Generated pressures were evaluated using the equation of state of MgO proposed by Ref. 27, which has the total residuals between the calculated and observed pressures of 0.8 GPa in root mean squares. X-ray

radiography was adopted to monitor the deformation of the high-pressure cell and measure the distance between the opposed anvils using a CCD camera.

The first and second runs were conducted using a uniaxial Kawai-type multi-anvil press with the Osugi-type guide block²⁸ (SPEED-MKII) installed at beamline BL04B1²⁹ and a six-ram press installed at beamline P61B, respectively. Six first-stage anvils were made of WC with 27-mm edge length, whereas eight second-stage anvils were made of SD with 14-mm edge length and 1.5-mm truncation. The grade of SD was “C-grade” by Sumitomo Electric Hard-metal Co. Ltd., which contains 8 wt. % Co as a binder. Note that the press loads of the six-ram press shown later in this paper are converted to those equivalent to the uniaxial press with an Osugi-type guide block.

The first run (M2661) was designed to examine whether ultrahigh temperature can be generated using a BDD heater with SD anvils. In order to realize this target more easily, the experiment was conducted at a relatively low pressure of ~25 GPa. We used a Cr-doped MgO octahedron (OMCR, Mino Ceramic Co., LTD.) with a 5.7-mm edge length as a pressure medium. To perfectly fit the edge of the octahedron pressure medium, we adopted sloped gaskets with a 3-mm width (the longer width), fixed on the eight anvils using a Tombow MONO MULTI Liquid Glue, for the lateral support of the pressure medium. The gaskets were made of natural pyrophyllite baked at a temperature of 1073 K for 30 min after shaping. Figure 1(a) shows a schematic drawing of the cell assembly for this run. To generate temperature efficiently, we used a small tubular heater (0.7/0.5 mm in outer/inner diameter), which was molded from a BDD powder with 3 wt. % boron. The heater was placed in a face-to-face direction of the octahedron. The BDD powder was prepared by grinding a high-pressure synthesized BDD block using a nano-polycrystalline diamond mortar.¹⁸ Packed TiC powders were used as electrodes. ZrO₂ sleeves were placed above and below the BDD heater to prevent quick thermal loss through the tops of SD anvils used as electrodes. A mixture of MgO and 10 wt. % diamond with 1 μ m grain size was used as a pressure marker. MgO and diamond powder were mixed in ethanol using an agate mortar. The role of the diamond is to suppress the grain growth of MgO during heating. Because the irradiated length in the beam direction is larger than the heater diameter. An Al₂O₃ tube was set outside the BDD heater to avoid the MgO diffraction out of the heater (pressure medium) from affecting that within the heater (pressure marker). A W₇₅Re₂₅–W₉₇Re₃ thermocouple of 0.05 mm diameter was placed at the sample center to monitor the temperature. Coils made of W₇₅Re₂₅–W₉₇Re₃ thermocouple wires (0.08 mm in diameter) were used to prevent thermocouple breakage during compression. W₇₅Re₂₅–W₉₇Re₃ thermocouple wires with a diameter of 0.13 mm were used as extension wires. The pressure effect on EMF of the thermocouple was ignored. The assembly was first compressed to a press load of 0.5 MN in 40 min and then to 1.0 MN in 30 min. The sample was pre-heated to 800 K and slowly cooled to room temperature at these press loads. The assembly was then compressed to a press load of 3.0 MN in 120 min for heating to 3000 K.

The second run (HH342) was designed to generate an ultrahigh pressure and temperature of 50 GPa and 3300 K simultaneously (Table I). One key point is whether ultrahigh pressure can be generated in the sample within the BDD heater, which has high

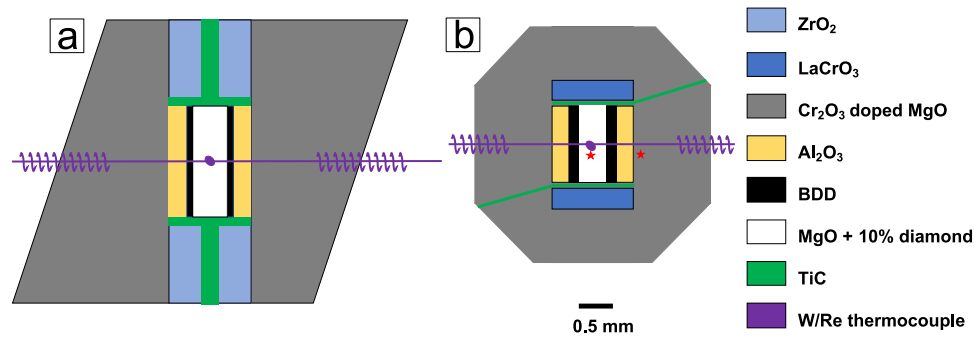


FIG. 1. Cell assemblies for experiments combining SD anvils and the BDD heater. [(a) and (b)] Cell assemblies used in Runs M2661 and HH342, respectively. For the cell assemblies [(a) and (b)], the BDD powder and CVD-BDD tube were used as heaters, respectively. The red stars in (b) mark the positions of pressure measurement by x-ray diffraction.

TABLE I. Summary of experiments using SD anvils and BDD heaters. Cell types a and b refer to the assemblies a and b in Fig. 1, respectively.

Run No.	Press	Cell type	Maximum load (MN)	Maximum pressure (GPa)	Maximum power (W)	Maximum temperature (K)
M2661	SPEED-MKII	a	3.0	25	367	3000
HH342	Six-ram press	b	6.0	52	1154	3300

strength. To increase the pressure generation efficiency, the edge lengths of the pressure medium and gasket width were reduced to 5.0 and 1.2 mm, respectively. Figure 1(b) shows a schematic drawing of the cell assembly for this experiment. Although the pre-synthesized high-pressure BDD was used in the first run, we used a CVD-synthesized BDD tube as a heater in this run because this type of BDD can be purchased commercially.¹⁹ A CVD-BDD block with a boron content of 0.5 wt. % (Changsha 3 Better Ultra-hard Materials Co. Ltd., China) was shaped into a tube using a green laser by Dutch Diamond Technologies BV. The heater axis was set in a corner-to-corner direction of the pressure medium. LaCrO_3 lids were placed on the TiC electrodes for thermal insulation. A mixture of MgO and 10 wt. % diamond (with $\sim 1 \mu\text{m}$ grain size) was packed inside the heater as a pressure marker. A $\text{W}_{75}\text{Re}_{25}$ – W_{97}Re_3 wire of 0.05 mm diameter was used as a thermocouple. The assembly was finally compressed to a press load of 6.0 MN. Before reaching this press load, the sample was pre-heated to 573, 1273, 1373, and 1763 K at press loads of 1.1, 1.9, 4.0, and 4.8 MN, respectively. To examine the diamond support, pressures were measured using MgO within and out of the BDD heater. Temperatures of the MgO out of the heater were assumed to be the same as those indicated by the thermocouple.

III. RESULTS AND DISCUSSION

A. Ultrahigh-temperature generation at pressures less than 30 GPa

Figure 2(a) shows the power–temperature relationship of the first run (M2661). The sample temperature almost linearly increased against the supplied power. The thermocouple worked at temperatures up to 2600 K, where the supplied power was 320 W. However, we were not able to measure temperatures above this temperature because the temperature indicated by the thermocouple started to

significantly stray away from the power–temperature relationship. We, therefore, estimated the temperatures above 2600 K by linearly extrapolating the power–temperature relationship obtained between 1800 and 2600 K. The highest temperature thus estimated was 3000 K at 367 W. It was therefore found that ultrahigh-temperature generation is possible using a cell assembly with SD anvils.

Figure 2(b) shows the pressure increase with increasing temperature at a press load of 3 MN. The pressure was 20.2 GPa before heating and increased with a rate of 1.8 MPa/K. The pressure reached 25.2 GPa at a temperature of 3000 K. The thermal pressure thus significantly increased sample pressures, which is a great advantage to use a BDD heater because sample pressures usually decrease with temperature when using cell assemblies with a LaCrO_3 or metal heater.^{7,11}

B. Diamond support of the BDD heater

Figure 3 shows the pressure generation history in run HH342 (the second run). It was found that the pressure generation efficiency was very low at the press load of 1.1 MN before heating. The pressure even decreased from 3 to 2 GPa by heating the sample to 573 K [Fig. 4(a)]. The pressure out of the heater was 17 GPa higher than that of the inside. These observations suggest that the pressure did not transmit to the inside of the heater due to the high strength of BDD.

At the load of 1.9 MN, the generated pressure inside the heater was still low, 6 GPa at ambient temperature (Fig. 3). The pressure difference between the inside and outside was even larger, 20 GPa [Fig. 4(b)]. During heating, the pressure inside increased non-linearly with a dramatic increase at the temperature range between 573 and 1173 K. At this temperature range, the pressure increased from 7.4 to 24.8 GPa, namely, at a rate of 30 MPa/K. At the

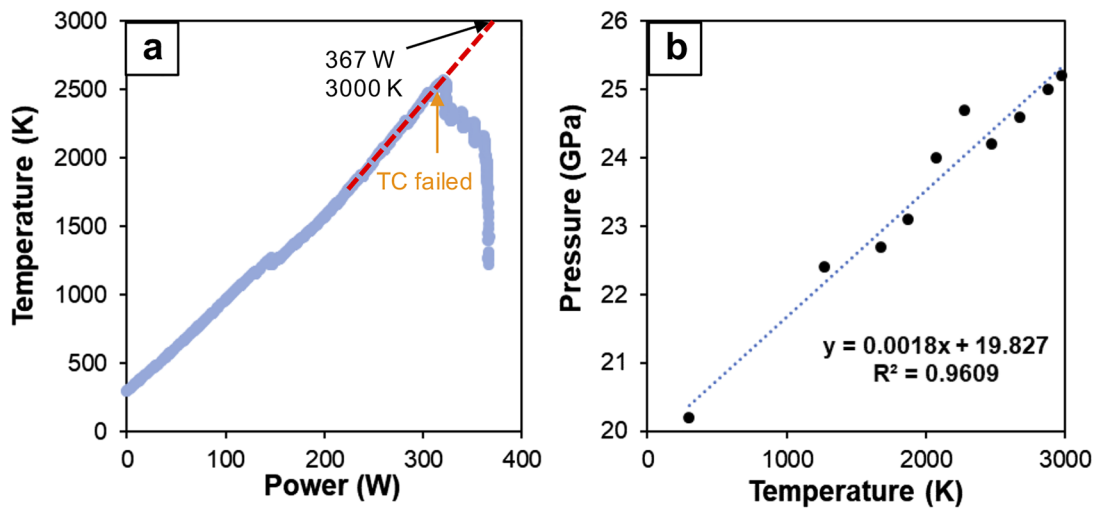


FIG. 2. Power–temperature (a) and temperature–pressure (b) relations in the first run (M2661). The orange arrow with the label “TC failed” marks the thermocouple failure at a temperature of 2600 K. The maximum heating power was 367 W, corresponding to 3000 K by linear extrapolation. The temperature values of data points with temperatures over 2600 K in (b) were estimated by their input power.

same time, the pressure difference decreased from 20.3 to 5.2 GPa, indicating the softening of BDD at high temperatures.

At higher loads, namely, above 3.0 MN, the pressure increased almost linearly with increasing temperature, at a rate of only 3 MPa/K. Unlike at a load of 1.9 MN, the pressure difference between the inside and outside increases slightly with increasing temperature, which may be caused by an increasing temperature difference between the inside and outside with increasing temperature. Therefore, the pressure increases by heating are considered to result from thermal pressure.

Interestingly, if we assume a thermal pressure of 3 MPa/K, the pressure increase (17.9 GPa) from 573 to 1173 K at 1.92 MN equals its decrease in pressure difference (15.1 GPa) plus the thermal pressure ($0.003 \times 600 = 1.8$ GPa) with a difference of 0.5 GPa. Namely, the dramatic increase in pressure at 1.92 MN should be caused mainly by the decrease in diamond support and partly by the thermal pressure. Thus, the BDD heater supported pressures up to 20 GPa at temperatures lower than 573 K, but the diamond support became insignificant at temperatures above 1173 K due to the high-temperature softening.³⁰

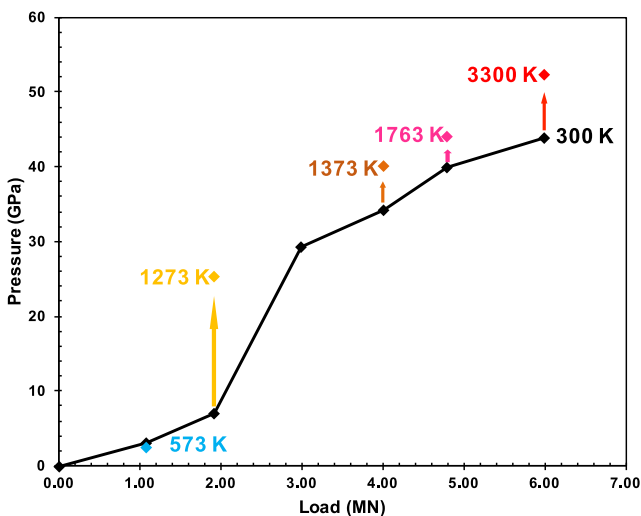


FIG. 3. Pressure–load relationship inside the BDD heater in the second run (HH342). The black line and markers indicate the pressures at 300 K. The colorful markers indicate the pressures at the highest temperature for each load.

C. Ultrahigh-pressure and -temperature generation

Figure 5 shows the power–temperature relationship of the last heating in the second run. Unfortunately, we were unable to read the thermocouple EMF at temperatures above 1800 K during heating due to large noises (probably from the heater or reaction between thermocouple and diamond). Interestingly, the thermocouple reading seemed to recover after cooling to 2673 K. The power–temperature relationships for heating and cooling below 1800 K are consistent with each other. The power–temperature curve shows a bend during cooling, which is commonly observed in BDD heaters,^{14,18–21} but shows approximately a linear shape during the heating. For a conservative estimate, we estimated the highest temperature at the maximum applied power (1154 W) to be 3300 K by linear extrapolation of the power–temperature relationship obtained up to 1800 K.

We note that the heating efficiency of the second run (2.6 K/W) was found much lower than that of the first run (10 K/W). This is probably due to the following two reasons: (1) The thermal insulators above and below the BDD heater were much thicker in the first run than in the second run, and (2) the anvil tops used as electrodes in the first run were insulated in contrast to the second run

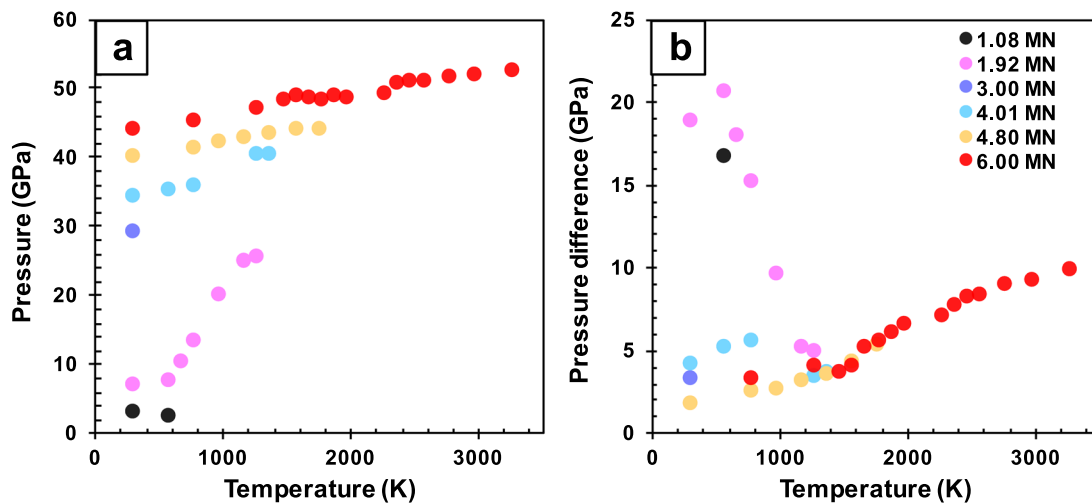


FIG. 4. (a) Pressure inside the BDD heater against the temperature at various press loads and (b) pressure difference between the outside and inside of the BDD heater against temperature at various press loads, in the second run (HH342). The numbers in the legend mark the press loads during heating. The temperature values of data points with temperatures over 1800 K were estimated by their input power using a linear relationship in Fig. 5.

due to the difference in the relative directions between the heater and anvil tops.

At the highest press load of 6 MN, the pressure monotonically increased with temperature and reached 48.2 GPa at 1773 K before the thermocouple failure. Based on the temperature estimation from the power–temperature relations, the pressure is considered to have

reached 50.4 GPa at a temperature of 2400 K. At this temperature, however, the diffraction peaks of MgO within the heater became very weak, probably due to the grain growth of MgO. Since we were still able to obtain diffractions from MgO out of the heater, we estimated the sample pressures at higher temperatures using a linear extrapolation based on the relationship of the pressures of the outside and inside of the heater obtained at lower temperatures (Fig. 6). This procedure leads to the pressure of 52.4 GPa at a temperature of 3300 K, which is agreed with the thermal pressure of 3 MPa/K obtained at lower temperatures [Fig. 4(a)]. Since the anvil gap at

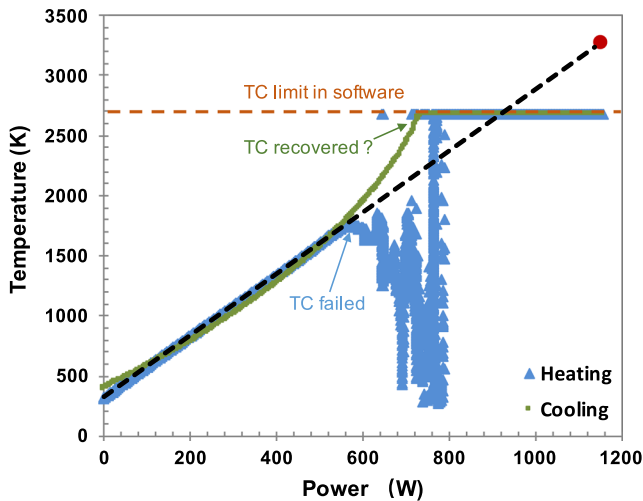


FIG. 5. Power–temperature relationship of the second run (HH342). The blue arrow with the label “TC failed” indicates the power and temperature at which EMF became unstable and the temperature reading was failed at about 1800 K. The orange dashed line marks the temperature reading limit (2673 K), which is the highest temperature calibrated at atmosphere pressure, in the heating software. Temperatures over the limit will be indicated as 2673 K. The green arrow with the label “TC recovered?” indicates that thermal couple reading may be recovered during cooling. The maximum applied power was 1154 W, corresponding to a temperature of 3300 K by the linear extrapolation (red circle).

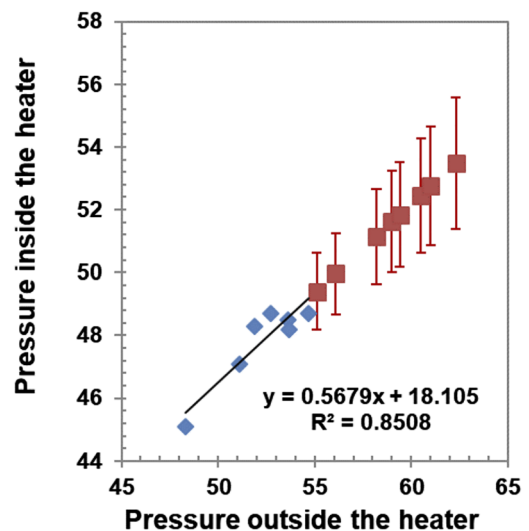


FIG. 6. Relationship between pressures of the inside and outside of the BDD heater in run HH342. The equation shows the linear fitting of data at temperatures between 300 and 1800 K. The red squares indicate predictions with a 95% confidential interval.

this press load is $\sim 100\ \mu\text{m}$, it is possible to generate higher pressure using the same assembly by applying a higher press load. Technologies of the tapered anvil, smaller anvil truncation, and hard SD anvil (such as “C2-grade,” Sumitomo Electric Hardmetal Co. Ltd.) will also facilitate high-pressure generation in future developments.

IV. CONCLUSIONS AND PERSPECTIVES

We succeeded in simultaneously generating an ultrahigh pressure and temperature of 50 GPa and 3300 K, respectively, using a BDD heater in combination with SD anvils in the multi-anvil apparatus. Even though the diamond support of the BDD heater significantly suppressed sample pressures at low temperatures, this support became insignificant at temperatures above 1200 K. This strategy will enable us to investigate the properties of minerals and rocks under lower-mantle conditions.

ACKNOWLEDGMENTS

The authors thank R. Njul for the preparation of materials of components of the high-pressure assemblies. The BDD powder was ground at the Geodynamics Research Center, Ehime University, under the PRIUS program with T. Irifune and T. Sinmei (Project Nos. A48, 2016-A02, 2017-A01, 2017-A21, and 2018-B30). L. Xie is aided by the postdoctoral fellowship of Bayerisches Geoinstitut, University of Bayreuth, Germany. This work received funding from the European Research Council (ERC) under the European Union’s Horizon 2020 Research and Innovation Programme (Proposal No. 787 527). The synchrotron radiation experiments were performed at the beamline BL04B1 of SPring-8 with the approval of the Japan Synchrotron Radiation Research Institute (JASRI) (Proposal Nos. 2017B1078 and 2018B1209). We also acknowledge DESY (Hamburg, Germany), a member of the Helmholtz Association HGF, for the provision of experimental facilities. Part of this research was carried out at the beamline P61B (Proposal No. I-20200114) with support from the Federal Ministry of Education and Research, Germany (BMBF, Grant Nos. 05K16WC2 and 05K13WC2).

The authors have no conflicts to disclose.

DATA AVAILABILITY

The authors declare that the majority of the data that support the findings of this study are available within the article. The unpublished data are available from the corresponding author upon reasonable request.

REFERENCES

- ¹A. M. Dziewonski and D. L. Anderson, *Phys. Earth Planet. Inter.* **25**, 297 (1981).
- ²D. Andrault, N. Bolfan-Casanova, G. Lo Nigro, M. A. Bouhifd, G. Garbarino, and M. Mezouar, *Earth Planet. Sci. Lett.* **304**, 251 (2011).
- ³G. Fiquet, A. L. Auzende, J. Siebert, A. Corgne, H. Bureau, H. Ozawa, and G. Garbarino, *Science* **329**, 1516 (2010).
- ⁴R. Nomura, K. Hirose, K. Uesugi, Y. Ohishi, A. Tsuchiyama, A. Miyake, and Y. Ueno, *Science* **343**, 522 (2014).
- ⁵E. Ito, *Miner. Phys.* **2**, 197 (2007).
- ⁶E. Ito, D. Yamazaki, T. Yoshino, H. Fukui, S. Zhai, A. Shatzkiy, T. Katsura, Y. Tange, and K.-I. Funakoshi, *Earth Planet. Sci. Lett.* **293**, 84 (2010).
- ⁷Y. Tange, T. Irifune, and K.-I. Funakoshi, *High Pressure Res.* **28**, 245 (2008).
- ⁸D. Yamazaki, E. Ito, T. Yoshino, N. Tsujino, A. Yoneda, X. Guo, F. Xu, Y. Higo, and K. Funakoshi, *Phys. Earth Planet. Inter.* **228**, 262 (2014).
- ⁹D. Yamazaki, E. Ito, T. Yoshino, N. Tsujino, A. Yoneda, H. Gomi, J. Vazhakuttiyakam, M. Sakurai, Y. Zhang, Y. Higo, and Y. Tange, *C. R. Geosci.* **351**, 253 (2019).
- ¹⁰T. Ishii, L. Shi, R. Huang, N. Tsujino, D. Druzhbin, R. Myhill, Y. Li, L. Wang, T. Yamamoto, N. Miyajima, T. Kawazoe, N. Nishiyama, Y. Higo, Y. Tange, and T. Katsura, *Rev. Sci. Instrum.* **87**, 024501 (2016).
- ¹¹T. Ishii, D. Yamazaki, N. Tsujino, F. Xu, Z. Liu, T. Kawazoe, T. Yamamoto, D. Druzhbin, L. Wang, Y. Higo, Y. Tange, T. Yoshino, and T. Katsura, *High Pressure Res.* **37**, 507 (2017).
- ¹²Z. Liu, M. Nishi, T. Ishii, H. Fei, N. Miyajima, T. B. Ballaran, H. Ohfuji, T. Sakai, L. Wang, S. Shcheka, T. Arimoto, Y. Tange, Y. Higo, T. Irifune, and T. Katsura, *J. Geophys. Res.: Solid Earth* **122**, 7775, <https://doi.org/10.1002/2017jb014579> (2017).
- ¹³T. Arimoto, T. Irifune, M. Nishi, Y. Tange, T. Kunimoto, and Z. Liu, *Phys. Earth Planet. Inter.* **295**, 106297 (2019).
- ¹⁴A. Shatzkiy, D. Yamazaki, G. Morard, T. Cooray, T. Matsuzaki, Y. Higo, K.-I. Funakoshi, H. Sumiya, E. Ito, and T. Katsura, *Rev. Sci. Instrum.* **80**, 023907 (2009).
- ¹⁵A. Yamada, T. Irifune, H. Sumiya, Y. Higo, T. Inoue, and K.-I. Funakoshi, *High Pressure Res.* **28**, 255 (2008).
- ¹⁶A. Yoneda, L. Xie, N. Tsujino, and E. Ito, *High Pressure Res.* **34**, 392 (2014).
- ¹⁷L. Xie, A. Yoneda, T. Yoshino, H. Fei, and E. Ito, *High Pressure Res.* **36**, 105 (2016).
- ¹⁸L. Xie, A. Yoneda, T. Yoshino, D. Yamazaki, N. Tsujino, Y. Higo, Y. Tange, T. Irifune, T. Shimai, and E. Ito, *Rev. Sci. Instrum.* **88**, 093904 (2017).
- ¹⁹L. Xie, A. Yoneda, Z. Liu, K. Nishida, and T. Katsura, *High Pressure Res.* **40**, 369 (2020).
- ²⁰K. Nishida, L. Xie, E. J. Kim, and T. Katsura, *Rev. Sci. Instrum.* **91**, 095108 (2020).
- ²¹L. Xie, *Rev. Sci. Instrum.* **92**, 023901 (2021).
- ²²T. Katsura, *Spec. Pap. Geol. Soc. Am.* **421**, 189–205 (2007).
- ²³B. Cochain, C. Sanloup, C. Leroy, and Y. Kono, *Geophys. Res. Lett.* **44**, 818, <https://doi.org/10.1002/2016gl071600> (2017).
- ²⁴L. Xie, A. Yoneda, D. Yamazaki, G. Manthilake, Y. Higo, Y. Tange, N. Guignot, A. King, M. Scheel, and D. Andrault, *Nat. Commun.* **11**, 548 (2020).
- ²⁵C. Sanloup, F. Guyot, P. Gillet, G. Fiquet, M. Mezouar, and I. Martinez, *Geophys. Res. Lett.* **27**, 811, <https://doi.org/10.1029/1999gl008431> (2000).
- ²⁶T. Sakamaki, E. Ohtani, S. Urakawa, A. Suzuki, and Y. Katayama, *Earth Planet. Sci. Lett.* **287**, 293 (2009).
- ²⁷Y. Tange, Y. Nishihara, and T. Tsuchiya, *J. Geophys. Res.*, **114**(B3), 1, <https://doi.org/10.1029/2008JB005813> (2009).
- ²⁸T. Ishii, Z. Liu, and T. Katsura, *Engineering* **5**, 434 (2019).
- ²⁹T. Katsura, K.-I. Funakoshi, A. Kubo, N. Nishiyama, Y. Tange, Y.-I. Sueda, T. Kubo, and W. Utsumi, *Phys. Earth Planet. Inter.* **143**, 497 (2004).
- ³⁰D. J. Weidner, Y. Wang, and M. T. Vaughan, *Science* **266**, 419 (1994).